Enhanced Differentiation of Human Embryonic Stem Cells Toward Definitive Endoderm on Ultrahigh Aspect Ratio Nanopillars

*Camilla Holzmann Rasmussen, Paul M. Reynolds, Dorthe Roenn Petersen, Mattias Hansson, Robert M. McMeeking, Martin Dufva, and Nikolaj Gadegaard**

Differentiation of human embryonic stem cells is widely studied as a potential unlimited source for cell replacement therapy to treat degenerative diseases such as diabetes. The directed differentiation of human embryonic stem cells relies mainly on soluble factors. Although, some studies have highlighted that the properties of the physical environment, such as substrate stiffness, affect cellular behavior. Here, mass-produced, injection molded polycarbonate nanopillars are presented, where the surface mechanical properties, i.e., stiffness, can be controlled by the geometric design of the ultrahigh aspect ratio nanopillars (stiffness can be reduced by 25.000×). It is found that tall nanopillars, yielding softer surfaces, significantly enhance the induction of definitive endoderm cells from pluripotent human embryonic stem cells, resulting in more consistent differentiation of a pure population compared to planar control. By contrast, further differentiation toward the pancreatic endoderm is less successful on "soft" pillars when compared to "stiff" pillars or control, indicating differential cues during the different stages of differentiation. To accompany the mechanical properties of the nanopillars, the concept of surface shear modulus is introduced to describe the characteristics of engineered elastic surfaces through micro or nanopatterning. This provides a framework whereby comparisons can be drawn between such materials and bulk elastomeric materials.

1. Introduction

Human embryonic stem (hES) cells have the potential to generate all cell types in the body, and it is suggested that they could provide an unlimited source for cell replacement therapy to treat degenerative diseases, including diabetes mellitus. The directed differentiation of hES cells into mature insulin producing cells follows a stepwise protocol, mimicking the in vivo embryonic development. The first differentiation step for many of the desired mature cell phenotypes, including beta cells, is the generation of definitive endoderm cells (DE).[1,2] Today, several DE cell differentiation protocols, using soluble growth factors and small molecules, are targeting selected signaling pathways, including Wnt, TGFβ, and AKT/PI3.[3–6] The next differentiation step toward beta cells is the generation of pancreatic endoderm (PE), where the current differentiation protocols also rely on soluble factors, including bFGF and retinoic acid.[7–10] Thus, the majority of differentiation protocols of hES cells utilizing only soluble factors, whereas the physical environment is generally not taken into consideration. However, accumulating evidence suggests that mechanical properties of the microenvironment play a critical role in stem cell differentiation and during the in vivo development of an embryo.[11–16] Most of these studies have been performed on mesenchymal stem cells[11,17–21] whereas the field of directed differentiation of hES cells have been largely unattended. So far, lineage differentiation induced by topography has been demonstrated using

C. H. Rasmussen, Dr. D. R. Petersen, Dr. M. Hansson
Novo Nordisk A/S
Novo Nordisk Park
2760 Maaloev, Denmark
C. H. Rasmussen, Dr. M. Dufva
DTU Nanotech
Technical University of Denmark (DTU)
2800 Kgs. Lyngby, Denmark
Dr. P. M. Reynolds, Prof. N. Gadegaard
Division of Biomedical Engineering
School of Engineering
University of Glasgow
Glasgow G12 8LT, UK
E-mail: Nikolaj.Gadegaard@glasgow.ac.uk
Prof. R. M. McMeeking
Department of Materials
University of California
Santa Barbara, CA 93106, USA
Prof. R. M. McMeeking
School of Engineering
University of Aberdeen
King's College
Aberdeen AB24 3UE, UK
Prof. R. M. McMeeking
Department of Mechanical Engineering
University of California
Santa Barbara, CA 93106, USA

DOI: 10.1002/adfm.201504204

micro and nanotopographies for neurons[22] and mesenchymal stem cells.[23] Taking the mechanical properties of the niche or biomaterials into account may help obtaining efficient, fully defined and xeno-free differentiation protocols to obtain mature functional cells of the endoderm lineage.

The mechanical properties of a surface can be readily modulated using hydrogels, which was originally reported by Pelham and Wang.[24] They demonstrated the importance of surface rigidity to control epithelial cell migration and spreading. Furthermore, Engler et al. demonstrated how surface stiffness could be linked to the path of differentiation of mesenchymal stem cells.[11] Trappmann et al. showed that substrates having similar mechanical properties but which varied in porosity showed differences in the ability to direct the differentiation of epidermal stem cells.[25] Thus, despite the ease of regulating the mechanical properties of gels, the mechanical changes can be associated to other physical differences. In an alternative approach, Chen and co-workers used rubber-like material polydimethylsiloxane (PDMS) micropillars to regulate the effective mechanical properties of substrates.[26,27] By adjusting the height and diameter of the pillars, it is possible to vary the apparent elasticity in shear sensed by the cells according to the following equation[28]

$$k = \frac{3}{64}\pi E \frac{D^4}{L^3} \tag{1}$$

where k is the corresponding spring constant, D denotes the diameter, L is the length, and E is the Young's modulus of the material. In PDMS, assuming a modulus of 2.5 MPa,[26] a pillar with a diameter of 2 μm gives spring constant from 6454 nN μm^{-1} (stiffer surface) to 3 nN μm^{-1} (softer surface) by changing the height from 0.97 to 12.9 μm, respectively. Fu et al. demonstrated that a large spring constant (effectively stiffer material) led to osteogenic differentiation whereas the low spring constant (softer material) led to adipogenic differentiation of human mesenchymal stem cells,[26] which was in line with the results demonstrated by Engler et al.[11] Yet, to make an appropriate comparison between the two different model systems, it is necessary to find a common descriptor. Work carried out using, e.g., acrylamide gels or PDMS is typically characterized by the mechanical properties of the substrate using the Young's Modulus, E. Whereas the PDMS micropillar system[26,29] is characterized by the spring constant, k, of the microfabricated pillars. Thus we propose the following approach. We consider the force applied by the cells to be in-plane of the substrate and thus are better characterized by the effective shear modulus, $\overline{G}$, of the substrate. For a bulk system the shear modulus is given by

$$G = \frac{E}{2(1+\nu)} \tag{2}$$

where ν is the Poisson ratio of the material. On the other hand, a material with an array of micro- or nanopillars has an effective shear modulus which can be described by

$$\overline{G} = \frac{3}{16}\left(\frac{D}{L}\right)^2 f\overline{E} \tag{3}$$

where $\overline{E}$ is the Young's modulus of the bulk material from which the pillars are made and f is the surface coverage of the pillars. A full derivation of these equations is available in the Supporting Information. Equipped with these relationships it is now possible to make a more direct comparison between the two different model systems which is listed in **Table 1**.

While PDMS used in research is better defined than many hydrogels and is in general biocompatible and can be replaced with FDA (Food and Drug Administration) approved silicones, PDMS or corresponding silicone devices are not amenable for large volume production. By contrast, traditional engineering hard plastics such as polycarbonate (PC), polymethylmethacrylate, and polystyrene are suitable for high volume replication by, for example, injection molding. The challenge, however, is that the Young's modulus of PC is 2–3 GPa as compared to 2–4 MPa for PDMS. In previous work, we have demonstrated how it is possible to manufacture ultrahigh aspect ratio nanopillars in PC by injection molding. Here we fabricated arrays of 100 and 150 nm diameter PC pillars with heights between 500 and 2000 nm.[30] The corresponding spring constant for such nanopillars range from 5 to 1400 nN μm^{-1} – similar to that of the PDMS work by Fu et al.[26] Moreover the softest pillars have an effective shear modulus similar to that of a commonly used acrylamide hydrogel. In the present work we demonstrate that these polycarbonate injection molded nanopillar surfaces can

Table 1. Summary of nanopillar dimensions and calculated mechanical characteristics.

Sample	Diameter [nm]	Height [nm]	Calculated spring constant [nN μm^{-1}]	Effective shear modulus [kPa]
100 nm tall (soft)	100	2000	5	34.6
150 nm tall (intermediate)	150	1700	45	242
150 nm short (stiff)	150	500	1400	2800
Control (flat) (E = 2.35 GPa)	–	–	–	≈860 000
Bulk PDMS (E = 2.5 MPa)	–	–	–	1333
Fu et al.[26]	2000	12 900	3	2.6
Fu et al.[26]	2000	6100	26	11.4
Fu et al.[26]	2000	970	6454	452
Engler et al.[11] Acrylamide (E = 40 kPa)	–	–	–	13.7

be used to improve differentiation from embryonic stem cells to DE or PE cells. The reported data indicate that this could be a commercially viable way to improve differentiation yield.

2. Results

2.1. Fabrication and Mechanical Measurements of Nanopillar Substrate

Arrays of polymeric nanopillars were fabricated on a 25 mm × 25 mm sample by injection molding as previously described.[30] The dimensions of the nanopillars and their equivalent mechanical properties are provided in Table 1 together with commonly used model systems from the literature.

The dimensions were characterized by scanning electron microscopy (SEM) (diameter) and atomic force microscopy (height). The corresponding spring constant, of the nanopillars, given in Table 1, was calculated using Equation (1) and the Young's modulus of the PC (2.35 GPa provided at www.bayer.com). Oblique view SEM images of the different nanopillars can be seen in **Figure 1**. Given that the bulk shear modulus of polycarbonate is 650 times higher than that of PDMS, yet it is possible to reduce its effective value by up to 25 000 times through the fabrication of nanopillars.

2.2. DE Differentiation on Nanopillars

In order to see possible effects of nanopillars on DE differentiation, the following DE differentiation protocol was employed. Samples coated with fibronectin were seeded with pluripotent stem cells (Oct3/4 expressing cell,[31] expanded for 4 d, and subsequently sequentially exposed to Wnt3a and Activin A[3] to differentiate them toward DE[32] (**Figure 2**). The level of differentiation was followed by immunofluorescent staining for Oct3/4 (hES cell marker) and Sox17 (DE marker) respectively. The total number of cell nuclei was determined by staining the cells with a DNA-binding fluorescent dye (DAPI). Image analysis was carried out to determine the ratio of Oct3/4 and Sox17 positive cells.

At the point of seeding, all cells were Oct3/4 positive and were uniformly seeded across the entire sample. However, it was clear from samples fixed one day after seeding (day 1) that the areas with nanopillars exhibited a reduced adhesion of the cells, especially the soft and intermediate nanopillars (**Figure 3**). Higher magnification images are available in Figure S1 (Supporting Information). Moreover, cells attached to these had a distinctly different morphology from cells on the control surface (this is the flat area surrounding the nanopillared regions). They exhibited an elongated and aligned morphology with respect to the symmetry of the nanopillar pattern (Figure 3). After 4 d in culture, the hES cells had proliferated extensively, and the cell layer was confluent on the control surface. However, on the soft and intermediate nanopillars, cells only attached at the edge of the nanopillar area and in a few small tight clusters on the tall nanopillars (Figure 3). This indicated that the soft and intermediate nanopillars arrays did not favor hES (Oct3/positive) cell attachment or proliferation. Subsequently, the DE differentiation was initiated by priming the cells with Wnt3a. One day after Wnt3a priming (day 5) the first Sox17 positive cells started to appear at the border of the confluent cell layer on the soft nanopillars. Such early Sox17 induction was not observed in the flat control sample (Figure 3 and Figure S2, Supporting Information). The DE differentiation protocol was continued with the addition of Activin A for three days. After just one day with Activin A treatment (day 6), the previously empty space on the soft nanopillars was occupied by Sox17 positive cells (Figure 3).

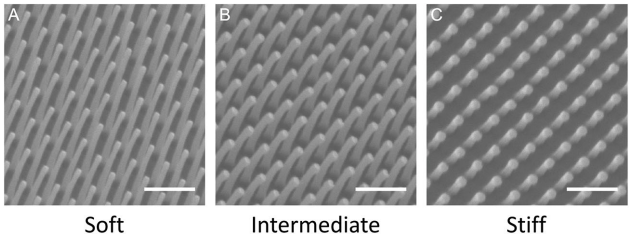

Figure 1. Scanning electron micrograph images of injection molded high aspect ratio nanopillars. A) Soft pillars – 100 nm diameter, 2 μm tall. B) Intermediate pillars – 150 nm diameter, 1.7 μm tall, and C) stiff pillars – 150 nm diameter, 0.5 μm tall. Scale bar: 1 μm, tilt: 25°.

To quantify cell numbers on each pillar array, we used the CellProfiler[33] software suite to measure the expression of both markers in each cell. Over 90% of the cells were Oct3/4 positive at day 1 (data not shown), but after 8 d of expansion and differentiation, cells on the softest pillars exhibited a far greater level of Sox17 positive cells as compared to both the control surface (≈50%) and the other nanopillar surfaces (<75%) (Figure S4, Supporting Information). This combined with images acquired at the interface between the flat region and the nanopillars (Figure S2, Supporting Information), makes it clear that the nanopillar arrays have a significantly larger proportion of Sox17 positive cells.

The quantification also showed that the number of cells from the initiation of the differentiation (day 4) declined throughout the differentiation on the flat control surface, whereas the cell number was steady on the intermediate and stiff nanopillars (**Figure 4**f). In contrast, the number of cells increased after the first day of Activin A treatment (day 5) throughout the rest of differentiation on the soft nanopillars (Figure 4f), which corresponds to what was observed from the microscope images (Figure 3). The ratio of Sox17 positive cells steadily increased

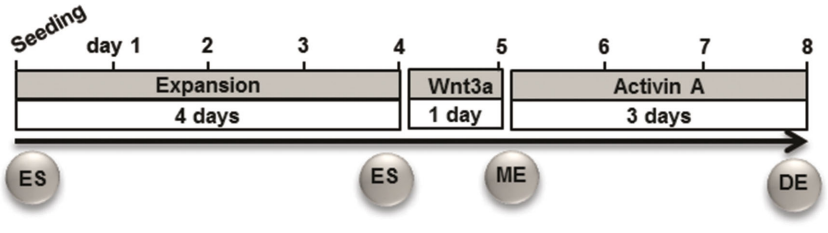

Figure 2. Schematic overview of the DE differentiation protocol used in this study. hESs cells were seeded and cultured for 4 d to allow expansion. The DE differentiation was initiated by priming the cells with Wnt3a which direct the cells toward mesendoderm. Subsequently 3 d exposure to Activin A directs the cells toward DE.

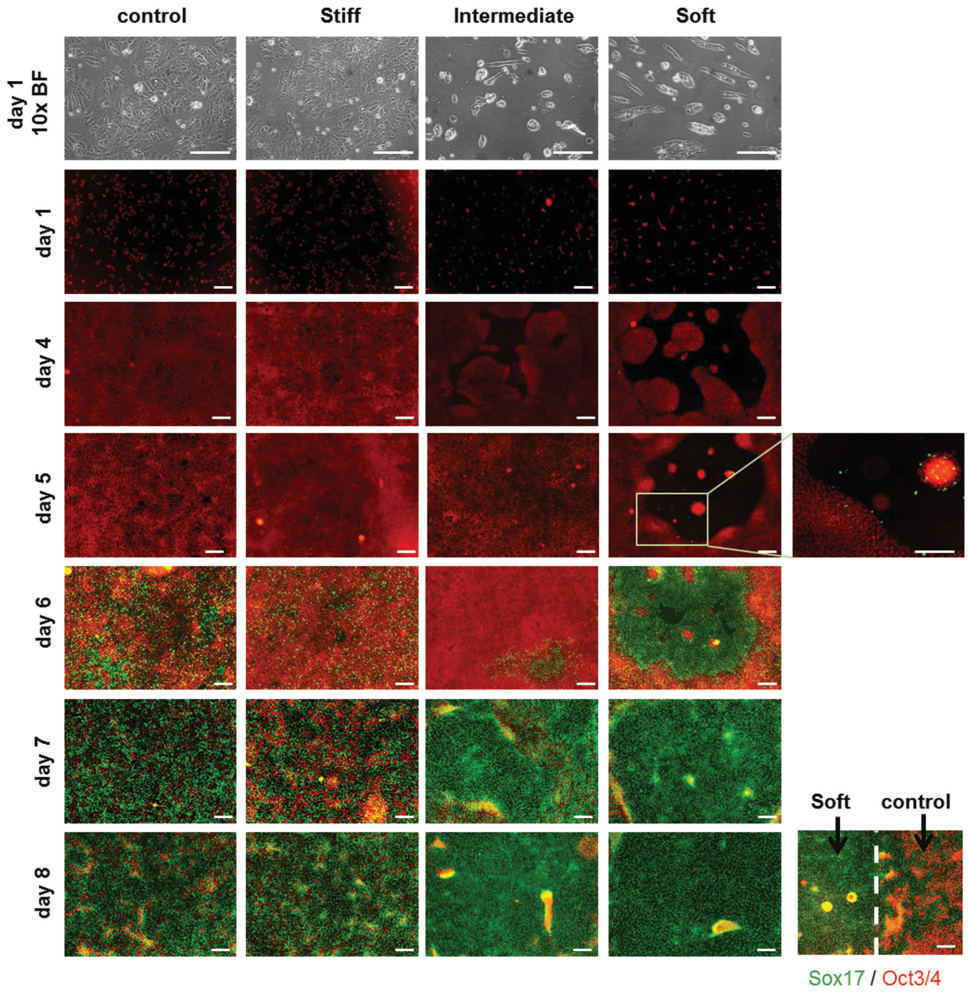

Figure 3. Top row: Phase contrast images of hES cells attached to nanopillar arrays after 1 d culture. On the control surface and stiff nanopillars, cells form a confluent monolayer. In contrast, fewer cells appear to adhere to the soft nanopillars, exhibiting a rounded morphology. Fluorescence microscope images (10×) of cells differentiating to DE at different time points on the nanopillars and the flat control surface. The cells were stained for Sox17 (green) and Oct3/4 (red). At day 5, after Wnt3a priming, Sox17 positive cells started to appear on the soft nanopillars (magnified insert at day 5). The difference in the DE induction between the flat control surface and soft nanopillars was obvious at the border at day 8. The images are acquired at the center of the nanopillared regions using a 4× objective, thus the interface between flat and structured regions is not visible. Scale bar = 200 µm.

throughout the differentiation on all substrates (Figure 4a–d). Already on day 6 nearly 50% of the cells are positive for Sox17 on the soft nanopillars as compared to 0% for the flat control (Figure 4). After 8 d, the conversion is nearly 100% on the softest substrate whereas we only observe ≈50% conversion on the control substrate. From the data, it is clear that the induction of Sox17 positive cells is more efficient on the nanopillar substrates as compared to the flat substrate.

2.3. Selectivity of a Heterogeneous Cell Population

In order to test if DE cells selectively attach to the nanopillars, a 1:1 mixture of ES cells and predifferentiated DE cells were seeded on the pillar arrays, and fixed the following day. There appeared to be no significant difference in the number of cells attached on nanopillars and the control surface. However, the ratio between DE and hES cells was higher on the softest nanopillars as compared to the control (**Figure 5**). It appeared that both Oc3/4 and Sox17 positive cells show tendencies to cluster to the respective cell type on the pillars but not on the flat surface (Figure 4). This indicates that the DE cells favor the pillars through either an initial attachment preference for DE cells or a subsequent migration during the 24 h incubation.

2.4. Pancreatic Endoderm Differentiation

The next differentiation step to PE was also investigated on the nanopillars. To allow an equal starting point for all surfaces, DE cells were produced using a highly effective differentiation protocol[9] in a cell culture flask and subsequently seeded on the nanopillar substrates. DE cells were differentiated to PE, using a 2 week differentiation protocol with bFGF.[9]

Subsequently the differentiated samples were fixed and stained for the PE markers Pdx1 and Nkx6.1.[34] Pdx1 and Nkx6.1 positive cells appeared in tight clusters with multiple cell layers (**Figure 6**). These clusters were significantly smaller on

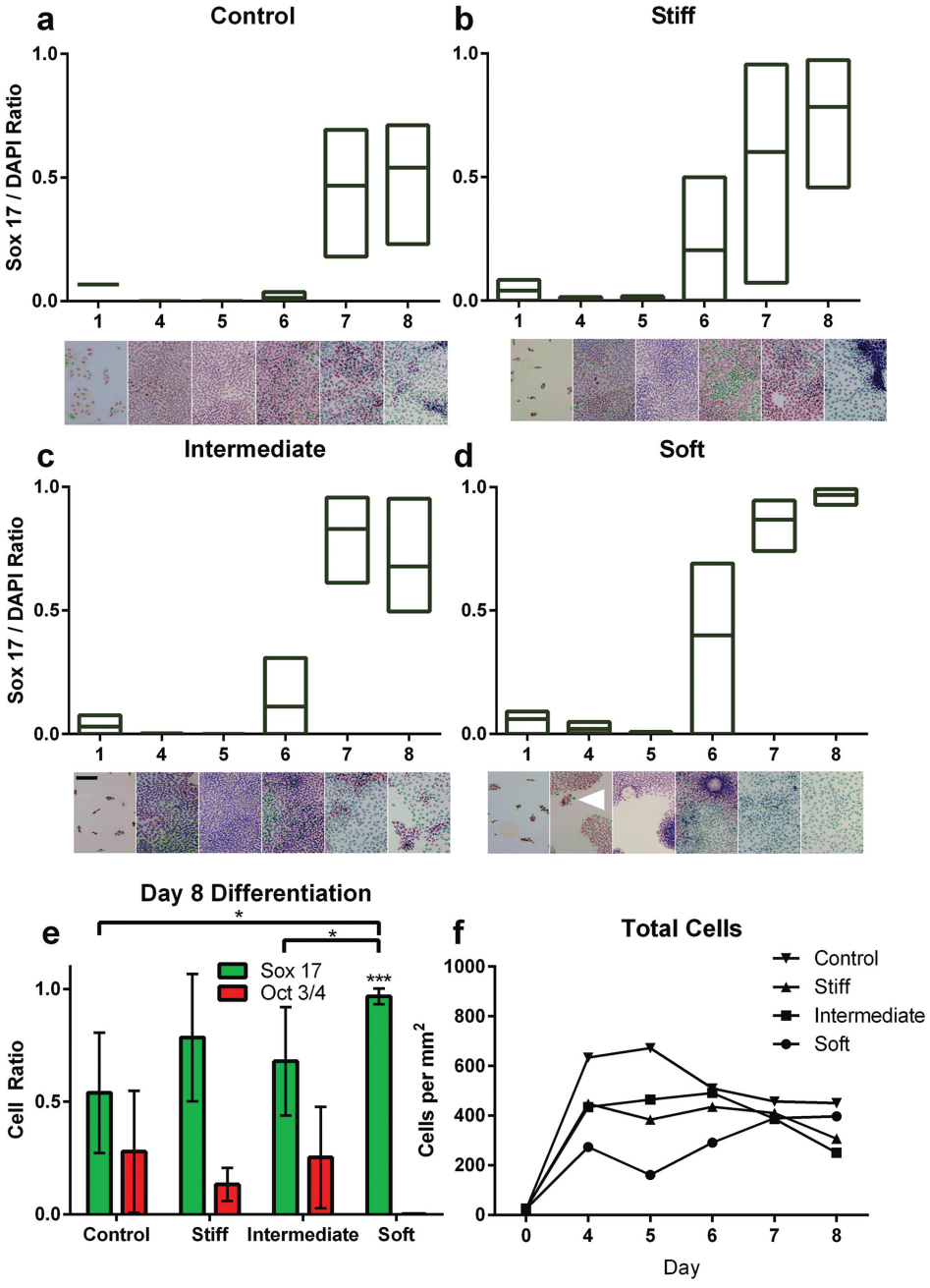

Figure 4. Differentiation of hES cells to DE cells on nanopillar arrays. a–d) Low-high bar graphs of Sox 17 positive cell ratio on nanopillars arrays. Boxes show the minimum, mean, and maximum value across $n = 3$. Representative images of each time point are inset below each graph. The softest nanopillars show a more consistent differentiation to a near-homogeneous population of Sox 17 cells. The white arrow in (d) indicates emergence of Sox 17 positive cells at day 4 on the soft pillar array – earlier than on the other nanopillars geometries. e) Comparison of the ratio of differentiated cells after 8 d culture. The softest nanopillars yield a cell population which is almost entirely differentiated (>97%) compared to the control surface. Results are mean ± SD, $n = 3$, $*p < 0.05$ by t-test, $***p < 0.001$ from control by ANOVA. f) Cell density on each nanopillars array and control surface after 8 d.

the nanopillars compared to the flat control (Figure 6). In contrast to DE differentiation, there appeared to be no correlation between the pillar elasticity and the PE induction (Figure 6). The percentage of Pdx1 positive cells was generally lower on the nanopillars compared to the flat control surface (Figure 6). This indicated that the PE differentiation required stiffer substrates such as the flat control surface.

3. Discussion

Several studies have demonstrated that cellular behavior, including cell differentiation, is affected by the mechanical properties of the environment.[11,17–23] However, these studies were performed with mesenchymal and adult stem cells. Here we have demonstrated that nanopillars greatly influence the

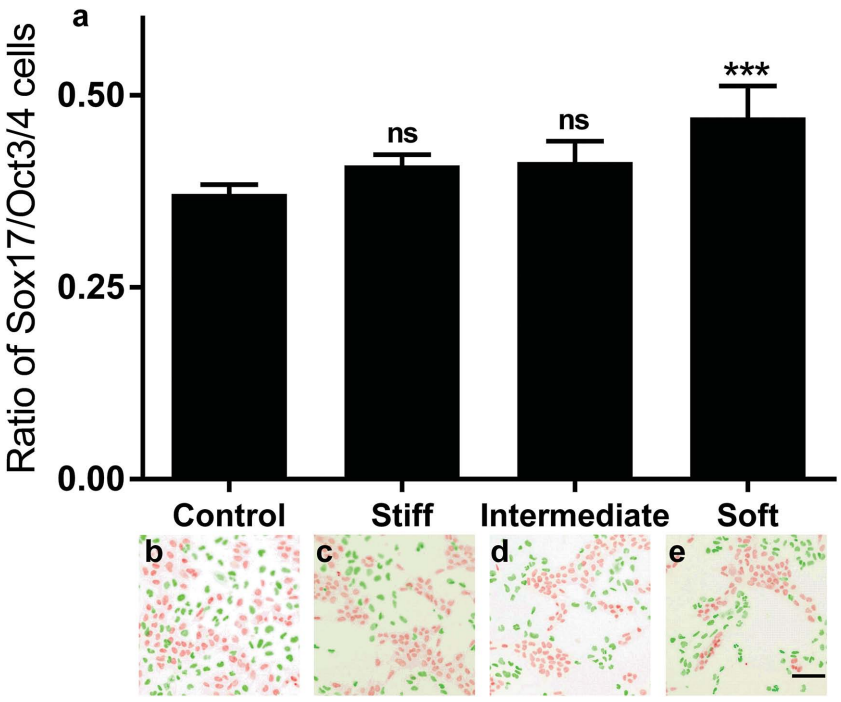

Figure 5. Comparison of the ratio of Sox17 positive cells attached compared to the control, 1 d after seeding heterogeneous cell populations (50:50 of Oct3/4:Sox17 positive cells). Red = Oct3/4 and green = Sox17. Fluorescent images have been color inverted for clarity. Values plotted as mean ± SD, ***$p < 0.001$ by ANOVA versus control, $n = 3$, Scale bar = 50 µm.

differentiation of human embryonic stem cells to DE. To our knowledge it has not previously been reported that mechanical properties of the surface influence the differentiation of hES cells toward specific lineages. The soft nanopillars had significantly higher percentage of Sox17 positive cells (94%) compared to the flat control surface (48%) after differentiation (Figure 3). Our studies suggest that the increased percentage of Sox17 positive cells is due to a combination of factors including surface dependent selective attachment, early and fast induction of Sox17 positive cells on the soft nanopillars.

On day 5, hES cells were located at the edge of the nanopillar area whereas the middle of the nanopillar area was almost empty with only a few clusters of hES cells (Figure 3). The previously empty space was occupied by Sox17 positive cells after only one day of Activin A treatment (day 6 from differentiation start). Such a fast repopulation of the nanopillar areas suggests that Sox17 cells migrated toward the nanopillars while the hES cells (Oct3/4 positive cells) were mainly restricted to the rigid control surface. Furthermore, the total cell number on soft nanopillars increased with time while the total number of cells decreased on the surrounding flat surface (Figure 4), which indicates a directed movement of cells from the flat surface toward the pillar region or cell proliferation. DE cells may have a slightly higher affinity to the pillar substrates compared to hES cells (Figure 5). Selective cell attachment using nanotopography has previous been reported between different cell types,[35,36] but to our knowledge it has not been observed between hES cells and hES cell derived DE cells. The selective affinity alone however cannot explain the high fraction of Sox17 on the soft nanopillars (Figure 3) because the ratio of hES to DE cells is ≈1:20 after the differentiation on soft pillars and only 1:1.29 using predifferentiated cells (Figure 5). Taken together, a reasonable line of events (**Figure 7**) is that hES cells preferentially grow on flat surfaces (Figures 3 and 4) leaving soft pillar surfaces almost empty. DE cells preferentially grow on softer nanopillars, and a potential mechanism to move into the area is by migration through durotaxis. The latter suggestion is strengthened by the observation that only the really high soft pillars had DE cell accumulation while the shorter harder pillars had an intermediate effect on DE cell accumulation. This suggests that the soft high pillars work as enrichment sites for DE cells. In contrast to the DE cells, PE cells preferred the harder surface indicating a selective advantage of DE cells on the soft pillars.

The observation that the differentiation was initiated very early on the soft nanopillars (Figure 3) indicates that the pillars may also directly and actively improve the outcome of Sox17 positive cells. Sox17 positive cells appeared already after the Wnt3a priming (day 5) on the soft nanopillars and such early induction was not seen on the flat control surface (Figure 3). Targeting the Wnt signaling using Wnt3a has previously been reported to increase the efficiency of mesendoderm specification, the transient stage prior the DE stage.[3,7,37] However, Sox17 is not expressed in mesendoderm but first later in the DE stage proper.[3,37] This indicated that the soft nanopillars together with the Wnt3a provided sufficient signals to differentiate the hES cells all the way to the DE stage and to not stop at the transient mesendoderm stage. One possible mechanism could involve the TGF-β pathway. The intracellular proteins YAP (Yes-associated protein) and TAZ (transcriptional coactivator with PDZ-binding motif) are involved in mechanotransduction[38] and these proteins are situated at the center of the TGF-β signaling pathway.[39] The TGF-β signaling pathway activated though Nodal/Activin A during the DE formation.[40] Thus, the soft nanopillars may provide mechanical signals to activate the TGF-β signaling pathway.

The migration capabilities of DE cells are consistent with the literature describing the development of an embryo and in vitro DE differentiation. In the early development of an embryo the DE is generated by epiblast cells undergoing EMT (epithelial to mesenchymal transition). The cells delaminate from the epiblast epithelial layer, break through the embryonic basement membrane and migrate through the primitive streak, where they will go through a mesendoderm transition state and subsequently become DE cells.[2,41] EMT has also been reported in the in vitro differentiation of hES cells to DE.[37] Our observations suggest a directed migration of DE cells, which is also observed in vivo during gastrulation. In vivo the migration through the primitive streak is guided by cues from the extracellular matrix and soluble factors.[42]

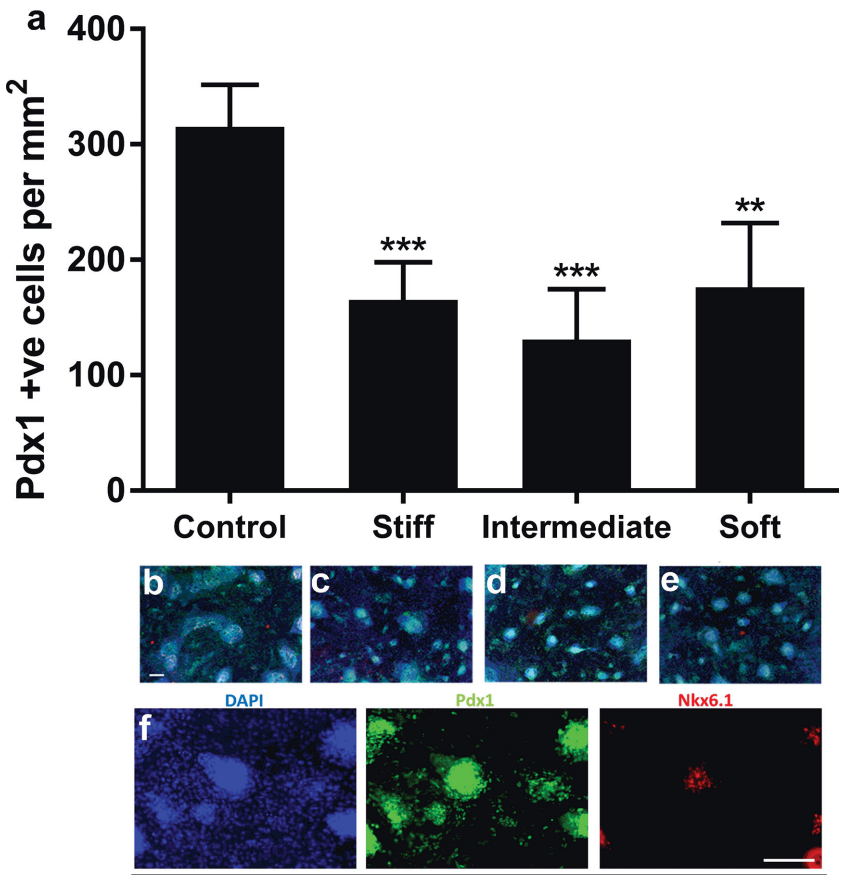

Figure 6. Comparison of Pdx1 positive cell number on nanopillar surfaces versus flat control after induced differentiation. a) Fewer Pdx1 positive cells emerge from DE differentiated cell colonies on all pillar arrays independent of stiffness as compared to the control surface. Engineering the perceived stiffness of the substrate using nanopillar arrays yields fewer differentiated cells. Values plotted as mean ± SD, $^{**}p < 0.01$, $^{***}p < 0.001$ by ANOVA versus control, $n = 3$. b–f) representative 4× and 10× fluorescence microscope images of cells differentiating from DE toward PE on the nanopillar surface and the flat control surface. DNA = blue, Pdx1 = green, and Nkx6.1 = red. Clusters of differentiating cells were found to be smaller on all three nanopillar surfaces when compared to flat controls. Lower panel shows representative 10× images of PE differentiation on soft nanopillars. Scale bars = 200 μm.

In contrast to the DE differentiation the PE differentiation was repressed by the nanopillars (Figure 6). This indicated that the DE and PE differentiation had different mechanical requirements of the environment. In published stem cell differentiation protocols, soluble molecules are added in different concentrations at different time points to mimic the stepwise embryonic development.[43] Likewise, the physical microenvironment changes during embryonic development,[44] and hereby the different differentiation steps may require different physical environments. Further the expression of the mechanical cell receptors integrins changes during stem cell differentiation.[45] Together with our results this suggests that the mechanical requirement for the environment changes throughout the different differentiation steps.

Our results demonstrate that nanopillars with shear modulus constant can be used as model substrates with different stiffness. Previous studies using hydrogels with different stiffness have demonstrated that cellular behavior including stem cell differentiation is influenced by the mechanical properties of the cell culture substrate.[11] However, other papers have suggested that the mechanical properties of the gel are not the only factors regulating fate.[25] Using a similar approach as Chen and co-workers with pillars to regulate the effective mechanical properties of substrates,[26,27] we were able to regulate the apparent stiffness of the PC substrate. We manufactured the PC nanopillars sample with injection molding, which is a highly reproducible and high content production method. Furthermore, the nanopillar arrays provide a fully defined synthetic surface for differentiation, which can be used for GMP (good manufacturing practices) compliant production of cells. Our findings suggest that DE differentiation can be significantly increased using soft nanopillars. Thus, taking the mechanical properties of the surface into account can improve the differentiation of hES cells. These findings can potentially also be used to develop a surface which can either purify DE cells or improve DE differentiation. One suggestion is to have areas of blank surfaces, which allow hES cells to attach and proliferate, and surrounding surfaces with nanopillars, where the DE cells migrate into.

4. Conclusion

Using mass produced, nanoengineered substrates we have been able to affect the differentiation of hES cells to DE and PE. More importantly we have observed that by providing a softer substrate interface, DE differentiation rate and efficiency were significantly higher than on the flat control surface. However, the underlying mechanism for the surface stiffness effect on the in

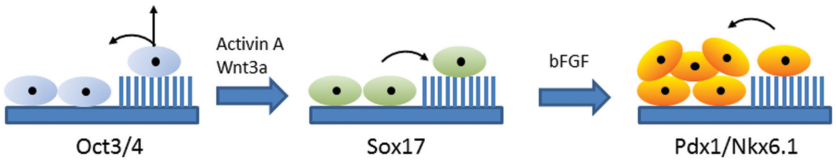

Figure 7. Proposed mechanism for mechanotransduction driven differentiation on nanopillared surfaces. The nanopillars provide a significant reduction of the effective shear modulus in comparison to the control substrate, which have a rigid character. Undifferentiated hES cells (Oct3/4 positive cells) favor the rigid surface and a limited number of cells will attach and proliferate on the elastic nanopillars. In contrast, when differentiating these hES cells to DE, Sox17 positive cells (DE cells) start to migrate into the nanopillars whereas the undifferentiated hES cells (Oct3/4 positive cells) will stay within the blank surface. In contrast, when differentiating DE to PE the nanopillars will reduce the formation of PE cells (Pdx1 and Nkx6.1 positive cells).

vitro differentiation remains unsolved and further studies are required. This engineered matrix provides a highly reproducible, synthetic and GMP compliant environment to achieve efficient differentiation of human embryonic stem cells to definitive endoderm.

5. Experimental Section

Fabrication of the Nanopillars: The fabrication of the UHAR (ultra-high aspect ratio) nanopillar samples has previously been described.[30] In brief, nanofabricated master inlays were made by a combination of electron beam lithography and reactive ion etching. The inlays were then used in an injection molding process whereby 100–1000 s of substrates have been made for the experiments. Macrolon OD2015 from Bayer was used was feedstock. Prior to cell seeding the samples were briefly oxygen plasma treated, 20 s at 40 W, to improve adhesion of the cells. The samples were placed in six-well plates (Nunc) and sterilized with 70% ethanol for 30 min and washed three times with phosphate buffered saline (PBS) (Gibco). Prior cell seeding, the samples were coated with 50 µg mL^{-1} fibronectin (Sigma) in PBS for 30 min at 37 °C in the cell incubator. The fibronectin solution was removed immediately before the seeding of cells.

Cell Culturing and Differentiation: The hES cells (SA121, Takara Bio Europe AB) were cultured in the feeder-free and defined DEF-CS500 system according to instruction from the supplier (Takara Bio Europe AB). The hES cells were cultured and differentiated in a humidified incubator with 5% CO_2.

For the differentiation toward definitive endoderm on the nanopillars, the following differentiation protocol was used. Cells were dissociated into single cell suspension with TrypLE Select (Invitrogen) and seeded at 40 000 cells cm^{-2} in DEF medium with 5×10^{-6} M RockI (Sigma-Aldrich). Cells were kept undifferentiated for 4 d in DEF medium. The differentiation was initiated on day 4 by rinsing with RPMI16040 + Glutamax medium (RPMI - Roswell Park Memorial Institute) (Gibco) and the addition of 100 ng mL^{-1} recombinant mouse Wnta3 (R&D Systems) in basal medium, containing RPMI medium with 2% B27 minus insulin (Gibco) and 0.1% Pen Strep (Invitrogen). On day 5, the cells were rinsed with RPMI medium and 10 ng mL^{-1} Activin A (Peprotech) in basal media was added. Fresh basal media with 10 ng mL^{-1} Activin A was added on day 6 and 7 and the differentiated was terminated on day 8. For the differentiation toward pancreatic endoderm the following protocol was used. The cells were first differentiated to definitive endoderm in fibronectin coated cell culture flask using a highly effective patented protocol (WO 2012175633 A1). Subsequently, the cells was rinsed with PBS and dissociated to single cell suspensions with TrypLE Select at room temperature. Seeding of the cells was performed with 200.000 cells cm^{-2} in basal media with 100 ng mL^{-1} Activin A and 5×10^{-6} M RockI. The cells was differentiated toward pancreatic endoderm with a 13 d published protocol with RPMI medium containing 64 ng mL^{-1} FGF2 (Peprotech), 12% knockout serum replacement (Gibco) and 0.1% pen strep.[9] Media was changed daily.

The attachment assay with heterogeneous cell population containing undifferentiated hES cells and DE cells was carried as follow. DE cells were derived with the patented differentiation protocol described above. DE and undifferentiated hES cells was mixed in the 50:50 ratio and seeded at 200.000 cells cm^{-2} in basal media with 100 ng mL^{-1} Activin A and 5×10^{-6} M RockI. The cells were incubated in the cell incubator overnight.

Immunofluorescence Staining and Microscopy: Fixation of the cells was performed by washing once with PBS and adding of 4% formaldehyde (Mallinsckridt Baker) for 20 min. The cells were washed with PBS and permeabilized 0.5% Triton-X-100 (Sigma-Aldrich) in PBS. The cells were again rinsed with PBS and blocked with TNB blocking buffer (0.1 M *tris*-HCL pH 7.5, 0.15 M NaCl, and 0.5% blocking reagent from Perkin Almer TSA (Tyramide Signal Amplification) kit) for 30 min. Primary antibodies were diluted in 0.1% TritronX-100 in PBS and applied to the cells, followed by incubation overnight at 4 °C. The following primary antibodies were used: goat polyclonal anti-Sox17 (1:1000) (R&D Systems, AF1924), mouse polyclonal anti-Oct3/4 (1:500) (Santa Cruz, sc5279), goat polyclonal anti-Pdx1 (1:8000) (Abcam, #ab47383), and mouse anti-Nkx6.1 (1:500) (Hybridoma bank, F55A10) (Klinck et al.[46]). Subsequently, cells were rinsed three times with PBS for 5 min. The secondary antibodies Alexa Fluor 594 conjugated donkey-antimouse IgG (Invitrogen) and Alexa Fluor 488 donkey-antigoat IgG (Invitrogen) were added in a 1:1000 dilution together with DAPI (4′,6-diamidino-2-phenylindole) (1:1000) (Sigma Aldrich) and occasional with Alexa Fluor 594 phalloidin (1:200) (Invitrogen) in 1% TritronX-100 in PBS for 45 min at room temperature. The cells were rinsed three times with PBS for 5 min.

Images were acquired using an Olympus CX41 upright microscope equipped with a prior motorized stage and 10× or 4× objective, operated by ImageProPlus (Media Cybernetics, UK). A total of 1026 images were processed, creating a dataset containing over 400 000 cells. The nuclear size and shape, along with intensity of DAPI, OCT4, and SOX17 markers within each nucleus, was measured using CellProfiler software suite (V2.1, Broad Institute, Harvard). Processing the full dataset took ≈6 h on an Intel Core i7 2600 CPU (central processing unit) @ 2.4 GHz with 16 Gb DDR2 RAM (random access memory) – this included various image measurements which were not used in the final analysis. The data were exported for processing and plotted using MATLAB.

Statistical Analysis: All values were presented as mean ± S.E.M. Data are presented for experiments performed at least as three independent experiments. For statistical analysis, ANOVA (analysis of variance) was used and a *p*-value of 0.05 was considered statistically significant.

Supporting Information

Supporting Information is available from the Wiley Online Library or from the author.

Acknowledgements

C.H.R. and P.M.R. contributed equally to this work. The authors would like to thank the staff and technicians of the James Watt Nanofabrication Centre for their assistance during the substrate fabrication process – particularly Dr. Johnny Stormonth-Darling. C.H.R. and M.D. acknowledge financial support from Innovation Fund Denmark and Novo Nordisk A/S, Denmark. N.G. acknowledges funding from EPSRC (Engineering and Physical Sciences Research Council, BBSRC (Biotechnology and Biological Sciences Research Council), MRC (Medical Research Council), and the Royal Society. Further N.G. and P.M.R. acknowledge funding from the Engineering and Physical Sciences Research Council (EPSRC) Grant EP/F500424/1 DTC (Doctorial Training Centre) in Cell and Proteomic Technologies (PR), and EC-funded project NAPANIL (Contract No. FP7-CP-IP214249-2).

Received: October 1, 2015
Revised: November 2, 2015
Published online: December 15, 2015

[1] O. D. Madsen, P. Serup, *Nat. Biotechnol.* **2006**, *24*, 1481.
[2] C. E. Murry, G. Keller, *Cell* **2008**, *132*, 661.
[3] K. A. D'Amour, A. D. Agulnick, S. Eliazer, O. G. Kelly, E. Kroon, E. E. Baetge, *Nat. Biotechnol.*, **2005**, *23*, 1534.
[4] M. Borowiak, R. Maehr, S. Chen, A. E. Chen, W. Tang, J. L. Fox, S. L. Schreiber, D. A. Melton, *Cell Stem Cell*, **2009**, *4*, 348.
[5] A. Kubo, K. Shinozaki, J. M. Shannon, V. Kouskoff, M. Kennedy, S. Woo, H. J. Fehling, G. Keller, *Development* **2004**, *131*, 1651.
[6] A. B. McLean, K. A. D'Amour, K. L. Jones, M. Krishnamoorthy, M. J. Kulik, D. M. Reynolds, A. M. Sheppard, H. Liu, Y. Xu, E. E. Baetge, S. Dalton, *Stem Cells* **2007**, *25*, 29.

[7] K. A. D'Amour, A. G. Bang, S. Eliazer, O. G. Kelly, A. D. Agulnick, N. G. Smart, M. a. Moorman, E. Kroon, M. K. Carpenter, E. E. Baetge, *Nat. Biotechnol.* **2006**, *24*, 1392.
[8] A. Rezania, J. E. Bruin, M. J. Riedel, M. Mojibian, A. Asadi, J. Xu, R. Gauvin, K. Narayan, F. Karanu, J. J. O'Neil, Z. Ao, G. L. Warnock, T. J. Kieffer, *Diabetes* **2012**, *61*, 2016.
[9] J. Ameri, A. Ståhlberg, J. Pedersen, J. K. Johansson, M. M. Johannesson, I. Artner, H. Semb, *Stem Cells*, **2010**, *28*, 45.
[10] M. C. Nostro, F. Sarangi, S. Ogawa, a. Holtzinger, B. Corneo, X. Li, S. J. Micallef, I. H. Park, C. Basford, M. B. Wheeler, G. Q. Daley, a. G. Elefanty, E. G. Stanley, G. Keller, *Development* **2011**, *138*, 1445.
[11] A. J. Engler, S. Sen, H. L. Sweeney, D. E. Discher, *Cell*, **2006**, *126*, 677.
[12] M. A. Conti, S. Even-Ram, C. Liu, K. M. Yamada, R. S. Adelstein, *J. Biol. Chem.* **2004**, *279*, 41263.
[13] K. Kurpinski, J. Chu, C. Hashi, S. Li, *Proc. Natl. Acad. Sci. USA*, **2006**, *103*, 16095.
[14] E. Farge, *Curr. Biol.* **2003**, *13*, 1365.
[15] K. Somogyi, P. Rørth, *Dev. Cell* **2004**, *7*, 85.
[16] A. Ranga, S. Gobaa, Y. Okawa, K. Mosiewicz, A. Negro, M. P. Lutolf, *Nat. Commun.* **2014**, *5*, 4324.
[17] M. J. Dalby, N. Gadegaard, R. Tare, A. Andar, M. O. Riehle, P. Herzyk, C. D. W. Wilkinson, R. O. C. Oreffo, *Nat. Mater.* **2007**, *6*, 997.
[18] R. J. McMurray, N. Gadegaard, P. M. Tsimbouri, K. V. Burgess, L. E. McNamara, R. Tare, K. Murawski, E. Kingham, R. O. C. Oreffo, M. J. Dalby, *Nat. Mater.* **2011**, *10* 637.
[19] M. J. Dalby, N. Gadegaard, R. O. C. Oreffo, *Nat. Mater.* **2014**, *13*, 558.
[20] K. A. Kilian, B. Bugarija, B. T. Lahn, M. Mrksich, *Proc. Natl. Acad. Sci. USA* **2010**, *107*, 4872.
[21] W. L. Murphy, T. C. McDevitt, A. J. Engler, *Nat. Mater.* **2014**, *13*, 547.
[22] S. Ankam, M. Suryana, L. Y. Chan, A. A. K. Moe, B. K. K. Teo, J. B. K. Law, M. P. Sheetz, H. Y. Low, E. K. F. Yim, *Acta Biomater.* **2013**, *9*, 4535.
[23] E. Kingham, K. White, N. Gadegaard, M. J. Dalby, R. O. C. Oreffo, *Small*, **2013**, *9*, 2140.
[24] R. J. Pelham, Y. L. Wang, *Biol. Bull.* **1998**, *194*, 348.
[25] B. Trappmann, J. E. Gautrot, J. T. Connelly, D. G. T. Strange, Y. Li, M. L. Oyen, M. A. Cohen Stuart, H. Boehm, B. Li, V. Vogel, J. P. Spatz, F. M. Watt, W. T. S. Huck, *Nat. Mater.* **2012**, *11*, 642.
[26] J. Fu, Y. K. Wang, M. T. Yang, R. A. Desai, X. Yu, Z. Liu, C. S. Chen, *Nat. Methods*, **2010**, *7*, 733.
[27] M. T. Yang, J. Fu, Y. K. Wang, R. A. Desai, C. S. Chen, *Nat. Protoc.* **2011**, *6*, 187.
[28] L. Lau, E. Lifschitz, *Theory of Elasticity*, Pergamon Press, Oxford, UK **1986**.
[29] S. Ghassemi, G. Meacci, S. Liu, A. A. Gondarenko, A. Mathur, P. Roca-Cusachs, M. P. Sheetz, J. Hone, *Proc. Natl. Acad. Sci. USA*, **2012**, *109*, 5328.
[30] J. M. Stormonth-Darling, R. H. Pedersen, C. How, N. Gadegaard, *J. Micromech. Microeng.* **2014**, *24*, 075019.
[31] J. Nichols, B. Zevnik, K. Anastassiadis, H. Niwa, D. Klewe-Nebenius, I. Chambers, H. Schöler, A. Smith, *Cell* **1998**, *95*, 379.
[32] M. Kanai-Azuma, Y. Kanai, J. M. Gad, Y. Tajima, C. Taya, M. Kurohmaru, Y. Sanai, H. Yonekawa, K. Yazaki, P. P. L. Tam, Y. Hayashi, *Development* **2002**, *129*, 2367.
[33] A. E. Carpenter, T. R. Jones, M. R. Lamprecht, C. Clarke, I. H. Kang, O. Friman, D. A. Guertin, J. H. Chang, R. A. Lindquist, J. Moffat, P. Goll, D. M. Sabatini, *Genome Biol* **2006**, *7*, R100.
[34] L. C. Murtaugh, *Development* **2007**, *134*, 427.
[35] W. Chen, L. G. Villa-Diaz, Y. Sun, S. Weng, J. K. Kim, R. H. W. Lam, L. Han, R. Fan, P. H. Krebsbach, J. Fu, *ACS Nano* **2012**, *6*, 4094.
[36] P. M. Reynolds, R. H. Pedersen, M. O. Riehle, N. Gadegaard, *Small* **2012**, *8*, 2541.
[37] S. Tada, T. Era, C. Furusawa, H. Sakurai, S. Nishikawa, M. Kinoshita, K. Nakao, T. Chiba, S.-I. Nishikawa, *Development* **2005**, *132*, 4363.
[38] S. Dupont, L. Morsut, M. Aragona, E. Enzo, S. Giulitti, M. Cordenonsi, F. Zanconato, J. Le Digabel, M. Forcato, S. Bicciato, N. Elvassore, S. Piccolo, *Nature* **2011**, *474*, 179.
[39] J. T. Morgan, C. J. Murphy, P. Russell, *Exp. Eye Res.* **2013**, *115*, 1.
[40] A. M. Zorn, J. M. Wells, *Annu. Rev. Cell Dev. Biol.* **2009**, *25*, 221.
[41] J. P. Thiery, H. Acloque, R. Y. J. Huang, M. A. Nieto, *Cell* **2009**, *139*, 871.
[42] S. F. Gilbert, *Developmental Biology*, 8th ed., Sinauer Associates Inc., MA **2006**.
[43] S. S. Kumar, A. A. Alarfaj, M. A. Munusamy, A. J. A. R. Singh, I. C. Peng, S. P. Priya, R. A. Hamat, A. Higuchi, *Int. J. of Mol. Sci.* **2014**, *15*, 23418.
[44] C. Bonnans, J. Chou, Z. Werb, *Nat. Rev. Mol. Cell. Biol.* **2014**, *15*, 786.
[45] J. C. Y. Wong, S. Y. Gao, J. G. Lees, M. B. Best, R. Wang, B. E. Tuch, *Cell Adhes. Migr.* **2010**, *4*, 39.
[46] R. Klinck, P. Serup, O. D. Madsen, M. C. Jørgensen, *J. Histochem. Cytochem.* **2008**, *56*, 415.